Heat shock transcription factor 1 preserves cardiac angiogenesis and adaptation during pressure overload

Jiming Li [1, 5, 6], Junbo Ge [1, 5*], Jie Yuan [1, 5], Hong Jiang [1, 5], Hong Ma [1, 5], Yanyan Liang [1], Yuhong Niu [1], Hui Gong [1], Ning Zhou [1], Aili Guang [1], Zhen Ma [1], Lingyan Yuan [1], Aijun Sun [1], Yuqi Wang [2*], Akira Nakai [3], Issei Komuro [4], Yunzeng Zou [1, 5*]

[1] Shanghai Institute of Cardivascular Diseases, Zhongshan Hospital and Institutes of Biomedical Sciences, Fudan University, 180 Feng Lin Road, Shanghai 200032, China

[2] Department of Vascular Surgery, Zhongshan Hospital, Fudan University, 180 Feng Lin Road, Shanghai 200032, China

[3] Biochemistry and Molecular Biology, Yamaguchi University School of Medicine, Minami-Kogushi 1-1-1, Ube 755-8505, Japan

[4] Department of Cardiovascular Science and Medicine, Chiba University Graduate School of Medicine, 1-8-1 Inohana, Chuo-ku, Chiba 260-8760, Japan

[5] These authors contributed equally to this work

[6] Present address: Department of Cardiology, Dong Fang Hospital, Jiaotong University, Shanghai, China

* Correspondence: zou.yunzeng@zs-hospital.sh.cn

Abstract

To examine how heat shock transcription factor 1 (HSF1) protects against maladaptive hypertrophy during pressure overload, we subjected *HSF1* transgenic (TG), knockout (KO) and wild type (WT) mice to a constriction of transverse aorta (TAC), and found that cardiac hypertrophy, functions and angiogenesis were well preserved in TG mice but were decreased in KO mice compared to WT ones at 4 weeks, which was related to *HIF-1* and *p53* expression. Inhibition of angiogenesis suppressed cardiac adaptation in TG mice while overexpression of angiogenesis factors improved maladaptive hypertrophy in KO mice. In vitro formation of vasculatures by microvascular endothelial cells was higher in TG mice but lower in KO mice than in WT ones. A siRNA of *p53* but not a *HIF-1* gene significantly reversed maladaptive hypertrophy in KO mice whereas a siRNA of *HIF-1* but not a *p53* gene induced maladaptive hypertrophy in TG mice. Heart microRNA analysis showed that *miR-378* and *miR-379* were differently changed among the three mice after TAC, and *miR-378* or siRNA of *miR-379* could maintain cardiac adaptation in WT mice. These results indicate that HSF1 preserves cardiac adaptation during pressure overload through *p53-HIF-1*-associated angiogenesis, which is controlled by *miR-378* and *miR-379*.

Introduction

Congestive heart failure is an end-stage of various heart diseases, which still accounts the reason for the high morbidity and mortality in many countries. However, the fundamental mechanisms of the development of heart failure have not yet been fully understood, thereby the potential strategies for the treatment of heart failure still need to be developed.

Heart failure is usually developed from a variety of heart diseases including cardiac hypertrophy [1]. Cardiac hypertrophy is the compensation for pressure overload [2]. Also, it is often an adaptation to exercises [3]. Although pressure overload-induced cardiac hypertrophy may have beneficial effects at the beginning to maintain cardiac function, it would ultimately develop to heart failure at chronic stage [4]. However, exercise-induced cardiac hypertrophy could maintain the adaptive state and normal function without progression to heart failure [3, 5]. Recently, we have reported that heat shock transcription factor 1 (HSF1), an important transcription factor for heat shock proteins and one of the highly conserved protective factor, plays a critical role in exercise-induced adaptive cardiac hypertrophy in mice [6]. In the study, expression of *HSF1* and its target molecule heat shock proteins was significantly upregulated in the heart by exercise but not by chronic pressure overload. HSF1 has protective roles against hypertrophy induced by chronic pressure overload in the *HSF1* transgenic mice. Overexpression of HSF1 in the heart prevented cardiomyocyte death and myocardial fibrosis in response to sustained pressure overload, thereby preserved cardiac function, and decrease of expression of *HSF1* in the heart impaired the adaptive response to exercise or acute pressure overload and thus caused cardiac dysfunction. On the other hand, it has been reported that

transcription of HSPs by HSF1 may be directly activated by pressure overload in the heart in both in vitro and in vivo models, which plays an important role in myocardial protection against cardiac overload [7]. It has also been reported that HSF1 activation and HSP72 gene transcriptional competence during simulated exercise are linked to elevated heart temperature and are not a direct function of increased cardiac workload [8]. However, whether and how HSF1 could protect against the transition of an adaptive cardiac hypertrophy to heart failure during a permanent pressure overload is still unclear.

Recently, we showed in our another study that cardiac angiogenesis induced by HIF-1 is crucially involved in the adaptive mechanism of cardiac hypertrophy and that impairment of cardiac angiogenesis by p53 accumulation induces transition of the adaptive cardiac hypertrophy to heart failure [9]. These data collectively suggest that there is a relationship between HSF1-regulated protection of cardiac function and HIF-1/p53-related angiogenesis in myocardium. In the present study, using a permanent pressure overload model by constriction of the aorta (TAC) in the *HSF1* transgenic (TG) or knockout (KO) mice and their littermate wild type (WT) mice, we demonstrated whether and how HSF1 preserves adaptation of the heart during a persistent cardiac workload.

Results

Overexpression of *HSF1* enhanced cardiac hypertrophy and functions during pressure overload in mice

To begin investigating the role of HSF1 as a cardiac protective factor during pressure overload, we performed the operation of TAC in the WT, *HSF1*-TG and -KO adult mice and observed the development of cardiac hypertrophy and changes in cardiac functions for 4 weeks. These mice were apparently healthy, and there were no significant differences in the body weight (BW), heart weight to BW ratio (HW/BW), or hemodynamic parameters, such as blood pressure (BP), heart rate (HR) and left ventricle (LV) end-diastolic pressure (LVEDP), among the three type mice before the TAC [6, 10] (data not shown). After TAC, BP was elevated by 40~50 mmHg similarly in the three types of mice, which was persistent for 4 weeks. However, cardiac hypertrophy and functions analyzed by echocardiography, catheterization and histology were quite different among the three mice. After TAC, cardiac hypertrophy was more significantly formed in the TG mice (Fig. 1b) but less in the KO mice (Fig. 1c) than in the WT ones (Fig. 1a). Although cardiac function was well preserved in the TG mice for 4 weeks, it was significantly decreased at 4 weeks in the WT mice while at 2 weeks in the KO ones after TAC (Fig. 1d). On the other hand, intercellular collagen content in myocardium was less in the TG mice but more in the KO mice than in WT mice after TAC (Fig. 1a-c). These results suggested that *HSF1* could enhance adaptive hypertrophy and preserve cardiac functions during a permanent pressure overload.

Overexpression of *HSF1* promoted cardiac angiogenesis after pressure overload

We next asked whether the role of *HSF1* is associated with an increase in angiogenesis in myocardium after pressure overload since angiogenesis is important for the development of cardiac hypertrophy [9]. Immunohistochemical staining of myocardial sections with an anti factor VIII-related antigen (von Willebrand factor, vWF), which specifically expressed in endothelial cells, revealed that the densities of vWF-positive vasculatures were higher in the heart of TG mice but lower in the heart of KO mice than those in the heart of WT mice after TAC (Fig. 2a), consisting with the results of cardiac hypertrophy. Inhibition of angiogenesis with an inhibitor TNP-470, significantly suppressed TAC-induced cardiac hypertrophy in the TG mice (Fig. 2b), while improving of angiogenesis by introducing the *VEGF* with *Ang-1* genes into the heart of KO mice could increase hypertrophy after TAC (Fig. 2c). These results indicated that the role of *HSF1* in maintaining the adaptive cardiac hypertrophy during pressure overload is associated with angiogenesis.

HSF1 induced reprogramming of expression of _HIF-1_ and _p53_ in the heart during pressure overload

Since we have recently reported that HIF-1-regulated angiogenesis is important for the development of pressure overload-induced cardiac hypertrophy and that p53-induced inhibition of HIF-1 causes the transition from cardiac hypertrophy to heart failure [9]. We therefore asked whether *HSF1* might induce angiogenesis through regulation of *HIF-1* and *p53* during pressure overload. There were no differences in expression of *HIF-1* and *p53* at basal condition before TAC (data not show). After TAC, consisting with our previous study [9], expression of *HIF-1* in WT heart was increased at early phase and

decreased from 2 weeks after TAC, and expression of *p53* was unchanged at early stage but elevated from 2 weeks after TAC (data not shown). However, expression of *HIF-1* was much higher in the TG heart but lower in the KO heart than that in WT one at 4 weeks after TAC (Fig. 3a). While expression of *p53* was not increased in the TG heart until 4 weeks after TAC, but it showed a higher level in the KO heart after TAC as compared with WT one (Fig. 3b). These results suggest that *HSF1* could regulate the expression of *HIF-1* and *p53* in heart during pressure overload.

HSF1 regulated expression of _HIF-1_ through _p53_ during pressure overload

To further elucidate the roles of *HIF-1* and *p53* in HSF1-related adaptive hypertrophy during pressure overload, we introduced a *HIF-1* gene or a small interfere RNA (siRNA) of *p53* into myocardium of the KO mice and a *p53* gene or a siRNA of *HIF-1* into myocardium of the TG mice, and performed TAC in these mice. Injection of the *HIF1* gene into heart did not affect maladaptive state of the KO mice after TAC, whereas TAC could induce an adaptive hypertrophy in the KO mice after downregulation of *p53* by the siRNA (Fig. 4a-c), indicating that at the deficiency of *HSF1*, injection of an extrinsic *HIF-1* gene could not exert roles while inhibition of the intrinsic *p53* might function during TAC. In the TG mice, however, introducing a *p53* gene into myocardium did not affect adaptive state after TAC, while TAC could induce a maladaptive hypertrophy after downregulation of *HIF-1* by the siRNA (Fig. 4d-f), indicating that in *HSF1*-overexpressing heart, effect of an extrinsic *p53* gene was abolished but inhibition of *HIF-1* by a siRNA was not interrupted. These results collectively suggest that *HSF1*-dependent effects on cardiac hypertrophy during TAC are relative to the regulation

of *p53* and *HIF-1* and that *HSF1* may regulate *HIF-1* through *p53*.

Endothelial cells were involved in *HSF1*-ralated protection of the heart during pressure overload

Since angiogenesis was significantly involved in the development of cardiac hypertrophy, we therefore asked whether *HSF1*-regulated protection of heart during pressure overload was due to the functions of microvascular endothelial cells (MEC). We cultured endothelial cells isolated from myocardium of adult WT, TG and KO mice and stretched them before implanted into matrigel. The abilities to form tube-like structures were not different among the three types of MEC without mechanical stretch (Fig. 5a). However, when mechanical stretch was imposed, the microvascular tubes were more formed by the MEC of TG mice but less by the MEC of KO mice than those by the MEC of WT mice (Fig. 5a). However, mechanical stress-evoked hypertrophic responses were not significantly different among the three types of cultured cardiomyocytes (data not shown). Also, after mechanical stretch, expression of *HIF-1* was significantly increased in MEC (Fig. 5b, c) but not in cardiomyocytes of the TG mice (data not shown), while expression of *p53* was significantly upregulated in the MEC (Fig. 5b, d) but not in cardiomyocytes of the KO mice (data not shown). These results indicate that the adaptive or the maladaptive cardiac hypertrophy observed in *HSF1*-TG or -KO mice, respectively, during pressure overload is, at least in part, related to the abilities of neovascularization by MEC but not to the hypertrophic responses of cardiomyocytes.

***miR-378* and *mi-R379* were regulators for cardiac *HSF1* during pressure overload.**

To explore the reason for the suppression of *HSF1* in myocardium after pressure overload, we employed a microRNA (miRNA) analysis in hearts of the WT, TG and KO mice after TAC for 2 weeks. Microarray showed 190 miRNAs significantly upregulated or downregulated in the WT heart after TAC, among which 10 were associated with the regulation of *HSF1* (data not shown). Furthermore, among the 10 miRNAs, only the expression of *miR-378* and *miR-379* was not changed among the three types of hearts without TAC (Fig. 6a). After TAC, however, *miR-378* was decreased in hearts of both the WT and the KO but increased in the TG heart, while *miR-379* was upregulated in hearts of both the WT and the KO but downregulated in the heart of TG mice (Fig. 6a). These results suggest that *miR-378* and *miR-379* might be related to the regulation of *HSF1* during TAC and that *miR-378* may be positively but *miR-379* negatively regulated the expression of *HSF1*

To confirm the data of miRNA array, we examined the expression of *miR-378* and *miR-379* in hearts of the WT, TG and KO mice after TAC using Northern blot method. Consisting with the results of miRNA array, *miR-378* was decreased but *miR-379* increased in the hearts of WT and KO mice, whereas *miR-378* was increased but *miR-379* decreased in heart of the TG mice (Fig. 6b, *left panels* and c). We also examined the expression of miRNAs in human hearts, and also found that *miR-378* was downregulated but *miR-379* upregulated in the failing heart compared to the heart without failure (Fig. 6b, *right panels*).

miR-378 and siRNA of _miR-379_ benefited the pressure-overloaded hearts

To test whether overexpression of *miR-378* or inhibition of *miR-379* could ameliorated a

maladaptive cardiac hypertrophy, we transfected the *miR-378* or a siRNA of *miR-379* into the myocardium of WT mice at 2 weeks after TAC and observed the development of cardiac hypertrophy and heart functions for another 2 weeks. At 4 weeks after TAC, the mice injected with *miR-378* or siRNA of *miR-379* showed a preserved cardiac hypertrophy and heart functions (Fig 6d), which was similar to those in the *HSF1* TG mice. Also, cardiac angiogenesis and *HSF1* expression was significantly increased in myocardium of the *miR-378* or siRNA of *miR-379*-transfected mice compared to those without the transfection (Fig. 6d, e). These results strongly suggest that *miR-378* and *miR-379* are regulators for *HSF1* in the heart and that upregulation of *miR-378* or downregulation of *miR-379* can ameliorate the maladaptive cardiac hypertrophy during pressure overload.

Discussion

Transition of the adaptive cardiac hypertrophy to a maladaptive one during hypertension is an important point to the development of heart failure [1, 2, 4, 9]. It is therefore necessary to explore a effective method to arrest the transition. In the present study, we found that overexpression of *HSF1* in the heart preserved adaptive hypertrophy and cardiac function through maintenance of cardiac angiogenesis during pressure overload; *HSF1* upregulated *HIF-1* through downregulation of *p53*; *miR-378*/*miR-379* were involved in the regulation of *HSF1* in pressure-overloaded heart in mice.

Although pressure overload-induced cardiac hypertrophy usually develops to heart failure eventually, exercise-induced cardiac hypertrophy does not [3, 5]. We have recently reported that the prolonged adaptive state of exercise-induced cardiac hypertrophy is regulated by HSF1 and HSPs, and that *HSF1*-TG mice do not develop to maladaptive cardiac hypertrophy under chronic pressure overload [6]. In the present study, we also showed that under a persistent pressure overload, overexpression of the *HSF1* in mice heart enhanced cardiac hypertrophy and delayed cardiac dysfunctions, while decrease of *HSF1* impaired adaptive cardiac hypertrophy and aggravated cardiac dysfunctions. However, the mechanism of how *HSF1*exerts on the heart has been still unclear although the protection of cardiomyocytes from death has been speculated [6]. We recently observed that inhibition of angiogenesis causes transition of an adaptive hypertrophy to cardiac dysfunctions during pressure overload [9] and that increases in cardiomyocyte death evaluated by a TUNEL method was observed from 2 weeks but not at early phase after pressure overload (unpublished data), suggesting that angiogenesis may play a role in protection of the heart by HSF1. In our present results, angiogenesis

was significantly more in the heart of *HSF1* TG mice but less in the heart of *HSF1* KO mice compared to WT heart after TAC. The changes of angiogenesis are paralleled to those of cardiac functions. Inhibition of angiogenesis by an inhibitor abolished preservation of cardiac adaptation in the *HSF1* TG mice, while overexpression of angiogenic factors in the heart of *HSF1* KO mice improved maladaptive hypertrophy under pressure overload. These results collectively show a pivotal role of angiogenesis in the beneficial effect of HSF1 on a workloaded heart.

HIF-1, a key transcription factor for the hypoxic induction of angiogenesis factors, can induce adaptive metabolic change as well as VEGF-mediated angiogenesis, which lead to the formation of new vessels [11, 12]. In the previous study, upregulation of HIF-1 expression and activation has been indicated to be important for the adaptive mechanism of cardiac hypertrophy at early phase during pressure overload [9]. In the present study, expression of *HIF-1* was higher in the TG heart but lower in the KO heart compared to the WT one after TAC, suggesting that *HSF1* may affect expression of *HIF-1*. However, overexpression of the *HIF-1* in the heart lacking *HSF1* did not benefit the maladaptive hypertrophy after TAC although overexpression of its downstream factors *Ang-1* and *VEGF* did improve the cardiac functions in the same type of mice, indicating that there might be another mechanism existing in the *HSF1* KO heart to suppress the effect of *HIF-1* but not that of its downstream factors during pressure overload. It has been reported that *HSF1* can act as a modifier of tumorigenesis through regulation of *p53*, which is required for tumor initiation and maintenance in a variety of cancer models [13]. It has also been indicated that p53 plays a critical role in the inhibition of adaptive upregulation of HIF-1 and angiogenesis during a chronic pressure overload [9], which

induces transition of cardiac hypertrophy to dysfunctions. In the present study, expression of *p53* was significantly downregulated in the *HSF1* TG heart but significantly upregulated in the KO one, while expression of *HIF-1* was significantly upregulated in the *HSF1* TG heart but downregulated in the KO one. Transfection of a siRNA into myocardium to knockdown the expression of *p53* rather than overexpression of a *HIF-1* gene significantly reversed the maladaptive hypertrophy in the KO mice whereas introduction of a siRNA of *HIF-1* but not a *p53* gene into the TG heart did worse the adaptive hypertrophy after TAC. These results collectively indicate that *HSF1* exerts effects on the cardiac angiogenesis after pressure overload through suppression of *p53* and thereby upregulating *HIF-1*, which leads to the adaptation maintenance of the pressure-overloaded heart.

It has been indicated that HSF1-regulated protection of heart is due to a direct protection of cardiomyocytes from death [6, 10, 14]. Sakamoto *et al.* indicated that the number of cardiomyocyte apoptosis was significantly less in the heart of *HSF1* TG mice compared with that of WT mice after pressure overload and that expression of transforming growth factor was markedly increased in the heart after pressure overload but was significantly prevented by overexpression of *HSF1* [6]. It is therefore thought that HSF1 prevents cardiomyocyte death by antagonizing the proinflammatory pathways, thereby preventing the transition from adaptive to maladaptive hypertrophy. Since angiogenesis also accounts for the development of cardiac hypertrophy [9], we therefore cultured MEC of hearts. Expression of *HIF-1* and that of *p53* were significantly observed in the MEC, but they were nearly undetectable in cardiomyocytes from the *HSF1* TG and the KO mice even after mechanical stretch (unpublished data). Meanwhile, the

vasculature formation was more significantly by the MEC of TG mice but less by the MEC of KO mice, whereas hypertrophic responses induced by mechanical stretch were similar between the two types of cardiomyocytes. These results collectively indicate that *HSF1*-associated long-term maintenance of adaptive cardiac hypertrophy is regulated by the MEC rather than by cardiomyocytes. These results also suggest a proper target cell for the treatment of heart failure.

It remains unclear how *HSF1* is downregulated under sustained pressure overload. Extracellular signal-regulated protein kinase (ERK) may increase HSF1 activity and participate in the activation of HSF1 in exercise-induced hypertrophy [6]. However, ERK has usually been known to be involved in abnormal growth of cells including pathological cardiac hypertrophy [15]. miRNAs are naturally existing, small, noncoding RNA molecules that downregulate posttranscriptional gene expression [16]. Their expression pattern and function in the heart has been recently demonstrated [17-21]. It has been shown that miRNAs play essential regulatory roles in the development of cardiac hypertrophy and that downregulation of *miR-1* is necessary for the relief of growth-related target genes from its repressive influence and induction of hypertrophy [17-19]. It has also been reported that *miR-133*, which belongs to the same transcriptional unit to *miR-1* and is decreased in mouse and human models of cardiac hypertrophy, has a critical role in determining cardiomyocyte hypertrophy [20]. However, these miRNAs are muscle relative that do not regulate cardiac angiogenesis. To explore the miRNAs targeting HSF1and angiogenesis in the heart, we performed a miRNA array of hearts in the *HSF1* TG, KO and WT mice after TAC for 2 weeks when transition of the adaptive hypertrophy to the maladaptive one initiates naturally [9]. Among the significantly changed

miRs relative to *HSF1*, *miR-378* was lower in the WT and KO but higher in the TG heart, whereas *miR-379* was higher in the WT and KO but lower in the TG heart, which is consistent with or contrast to the transcription levels of *HSF1* in the heart, respectively. *miR-378* has been reported to enhance cell survival, tumor growth, and angiogenesis through repression of the expression of two tumor suppressors, *Sufu* and *Fus-1* [22]. *miR-379* has been indicated to play an important role in neurogenesis in the placental mammals [23]. However, the role of them in the regulation of cardiovascular diseases has not yet been reported. Here, introduction of the *miR-378* or *siRNA* of *miR-379* into myocardium of the WT mice resulted in an upregulation of *HSF1* and angiogenesis, and a preservation of cardiac adaptation. These results indicate that *miR-378* and *miR-379* are also regulators for expression of *HSF1* during mechanical stresses and that they may be as target molecules to interrupt the transition of an adaptive cardiac hypertrophy to a maladaptive one. Future study will focus on how *miR-378* and *miR-379* regulate *HSF1* and whether there is a relationship between the two miRs in the regulation of *HSF1*.

In summary, we observed that overexpression of the *HSF1* in heart of mice induced an improvement of angiogenesis through downregulation of *p53* and subsequent upregulation of *HIF-1*, leading to a preservation of adaptive hypertrophy and cardiac functions and that *miR-378* and *miR-379* were involved in the regulation of *HSF1* expression in heart during a persistent pressure overload. Although further studies are required, upregulation of *HSF1* by promotion of *miR-378* and/or inhibition of *miR-379* in the heart may be a novel therapeutic strategy for preventing the transition from adaptive cardiac hypertrophy to heart failure.

Methods

Mice. Generation of the *HSF1* TG and KO mice has been previously described [24, 25]. Twelve-week-old male TG, KO and WT mice were used. There were no significant differences in BW, HW, HW to BW ratio (HW/BW), BP and HR among three types of mice at basal condition. All animal experimental protocols were approved by the Animal Care and Use Committee of Fudan University, and in compliance with guidelines for the Care and Use of Laboratory Animals published by the National Academy Press (NIH Publication No. 85-23, revised 1996).

Pressure-overload model. Strong pressure overload was imposed on the heart of mice by TAC operation as described previously [9]. In brief, mice were anesthetized by intraperitoneal injection of a cocktail of ketamine HCl (100 mg/kg) and xylazine (5 mg/kg) and artificially ventilated using a respirator. The transverse aorta was constricted together with a blunted 27-gauge needle, which was pulled out later. Haemodynamic measurements were taken by inserting a micronanometer catheter (Millar 1.4F, SPR 671, Millar Instruments) from the right common carotid artery into aorta and then LV. The transducer was connected to Power Laboratory system (AD Instruments, Castle Hill, Australia), and BP, HR, and LVEDP were measured.

Injection of the adenovirus vectors into myocardium of mice. Constructions of adenovirus vectors encoding *HIF-1*, *VEGF*, *Ang-1*and *p53* were as previously described [9]. Adenovirus vectors encoding *miR-378* were generated by PCR from mouse genomic DNA fragments (Invitrogen). siRNA of *p53* and *HIF-1* and their scramble RNA were

purchased from SantaCruz Biotechnology, Inc. siRNA of *miR-379* was purchases from Genepharma, Inc. (Shanghai, China). siRNAs were inserted into adenovirus vectors (Invitrogen). Infusion of the relative adenovirus vectors into myocardium through coronary artery was performed in some of WT, TG and KO mice 2 days before TAC as reported previously [9]. Efficacy of the transfection into myocardial evaluated by an X-gal staining of Ad. *LacZ* vector was ~50% (data not shown). Injection of the siRNA induced a significant knockdown (> 50%) of the relative mRNA evaluated by the RT-PCR in myocardium (data not shown).

miRNA microarrays. Adult WT, TG and KO mice were subjected to sham or TAC operation. Two weeks later, the animals in sham groups with normal BP (100~120 mmHg) and those in TAC groups with significant elevation of BP (40~50 mmHg) were enclosed. Low-molecular-weight RNA was isolated from cardiac tissue by using the mirVana miRNA Isolation Kit (Ambion, Austin, TX). RNA from three animals in each group was pooled and used for miRNA expression analysis by using the miRMAX microarray. A total of 186 miRNAs examined showed comparable relative expression at baseline. The miRNAs without changes among the WT, *HSF-1* TG and the KO hearts subjected to sham operation were selected for comparison. Differentially regulated miRNAs were defined as those with either < 0.5- or > 1.5-fold changes in expression compared the expression levels of sham hearts with TAC ones.

Northern blotting. Total RNA was extracted from heart tissues using TRIzol reagent according to the protocol of the manufacturer (Invitrogen). To aid analysis of miRNA,

polyethylene glycol was applied to remove large-sized RNA. Nothern blot analysis was performed as described elsewhere [26]. The microRNA Detection Probes of *miR-378* and *miR-379* were obtained from miRCURY LNA™ . The probes were 5'-end labeled with biotin using miRNA probe and marker kit and used for hybridization.

Human heart tisssues. We obtained the human heart tissues from the Zhongshan Hospital, Fudan University under the procedures approved by the Ethnic Committee for Use of Human Samples of the Fudan University. The LV tissues were from two rejected hearts of healthy persons during heart transplantation and from two explanted hearts of patients with end stage of heart failure.

Echocardiography. Transthoracic echocardiography was performed using an animal specific instrument (VisualSonics Vevo770, VisualSonics Inc. Canada) [6, 9]. Mice were weakly anesthetized and M-mode images of the LV were recorded when the mice partially recovered from anesthesia. All measurements were averaged for three consecutive cardiac cycles and were carried out by three experienced technicians who were unaware of the identities of the respective experimental groups.

Culture of cardiac myocytes and microvascular endothelial cells of mice. Cardiac myocytes and MEC were prepared from ventricles of 1-day-old neonatal WT, TG and KO mice. The cells were cultured in silicone dishes at a density of $1X10^5$ cells/cm^2 in Dullbecco modified Eagle medium (DMEM) supplemented with 10% fetal bovine serum (FBS) for CM and in 100-mm dishes at a density of $5X10^4$ cells/cm^2 in DMEM

supplemented with 20% FBS for MEC to grow to subconfluence as described elsewhere. The 2~3 passages of MEC were used for vascular formation experiments

Microvascular formation experiment. MEC were characterized by the immunocytochemistry staining with an anti vWF antibody and showed a purity of more than 95%. After 2-3 passages of culture, the MEC were resuspensed in 2% FBS-DMEM, implanted onto the matrigel (BD) in 24-well plate in a density of $5x10^4$ cells/well and grown for 18 hours. Some of MEC were subjected to a mechanical stretch for 30 min before implantation onto the matrigel. The capillary formation was observed under a microscope and quantified by calculating the number of tube-like structures in whole well.

Histological analysis. Heart tissues were fixed in 10% formalin and embedded in paraffin or frozen in cryomolds, sectioned at 4 μm thickness and stained with hematoxylin and eosin (H-E) for histological examination, Masson trichrome for fibrosis and anti vWF for vascular endothelial cells, respectively. Digital photographs were taken at magnification x25, x100, x400, x1000, respectively. For measurement, five random high-power fields from each section were chosen and quantified in a blinded manner. The extent of fibrosis and the densities of vasculatures were measured in 5 sections from each heart and the value was expressed as the ration of Masson trichrome stained area to total LV wall or as the number of blood vessels/mm^2, respectively.

Reverse transcription-polymerase chain reaction (RT-PCR) analysis. Total RNA was

isolated from the heart tissues or cells using TRIzol reagent (15596-018, Gibco BRL). The expression of the relative mRNA levels was evaluated using RT-PCR. The PCR products were subject to electrophoresis on 1.5% agarose gels, scanned, and semi-quantitated using Image-Quant software (Kodak 1D V3.53; Kodak, New Haven).

Statistics. Data are presented as mean ± S.E.M. Multiple group comparison was performed by one-way ANOVA followed by LSD procedure for comparison of means. Comparison between 2 groups under identical conditions was performed by the 2-tailed Student'*t* test. A value of $p < 0.05$ was considered statistically significant.

Acknowledgement

We want to thank Mr. Yao R and Ms Qian S for the excellent technical assistances. This work was supported by National Science Fund for Distinguished Young Scholars (30525018), National Basic Research Program of China (2007CB512003), China Doctoral Foundation (20060246079) and Science and Technology Commission of Shanghai Municipality (05XD14003).

References

1. Levy, D. *et al*. Prognostic implications of echocardiographically determined left ventricular mass in the Framingham Heart Study. *N. Engl. J. Med.* **322**, 1561-1566 (1990).
2. Frey, N. & Olson, E. N. Cardiac hypertrophy: the good, the bad, and the ugly. *Annu. Rev. Physiol.* **65**, 45-79 (2003)
3. Adams, T. D., Yanowitz, F. G., Fisher, A. G., Ridges, J. D., Lovell, K. & Pryor, T. A. Noninvasive evaluation of exercise training in college-age men. *Circulation* **64**, 958-965 (1981).
4. Katz, A. M. Cardiomyopathy of overload. A major determinant of prognosis in congestive heart failure. *N. Engl. J. Med.* **322**, 100-110 (1990).
5. Pelliccia, A. & Maron, B. J. Outer limits of the athlete's heart, the effect of gender, and relevance to the differential diagnosis with primary cardiac diseases. *Cardiol. Clin.* **15**, 381-396 (1997).
6. Sakamoto, M. *et al*. Upregulation of heat shock transcription factor 1 plays a critical role in adaptive cardiac hypertrophy. *Circ. Res.* **99**, 1411-1418 (2006).
7. Nishizawa, J., Nakai, A., Komeda, M. Ban, T. & Nagata, K. Increased preload directly induces the activation of heat shock transcription factor 1 in the left ventricular overloaded heart. *Cardiovasc. Res.* **55**, 341-348 (2002).
8. Staib, J. L., Quindry, J. C., French, J. P., Criswell, D. S. & Powers, S. K. Increased temperature, not cardiac load, activates heat shock transcription factor 1 and heat shock protein 72 expression in the heart. *Am. J. Physiol. Regul. Integr. Comp. Physiol.* **292**, R432-R439 (2007).

9. Sano, M. *et al*. p53-induced inhibition of Hif-1 causes cardiac dysfunction during pressure overload. *Nature* **446**, 444-448 (2007).
10. Zou, Y. *et al*. Heat shock transcription factor 1 protects cardiomyocytes from ischemia/reperfusion injury. *Circulation* **108**, 3024-3030 (2003).
11. Semenza, G. L. Targeting HIF-1 for cancer therapy. *Nat. Rev. Cancer.* **3**, 721-732 (2003).
12. Pugh, C. W. & Ratcliffe, P. J. Regulation of angiogenesis by hypoxia: role of the HIF system. *Nat. Med.* **9**, 677-684 (2003).
13. Dai, C., Whitesell, L., Rogers, A. B. & Lindquist, S. Heat shock factor 1 is a powerful multifaceted modifier of carcinogenesis. *Cell* **130**, 1005-1018 (2007).
14. Yan, L. J., Christians, E. S., Liu, L., Xiao, X., Sohal, R. S. & Benjamin, I. J. Mouse heat shock transcription factor 1 deficiency alters cardiac redox homeostasis and increases mitochondrial oxidative damage. *EMBO J.* **21**, 5164-5172 (2002)
15. Chien, K. R., Grace, A. A. & Hunter, J. J. Molecular biology of cardiac hypertrophy and heart failure. In: Chien KR, ed. *Molecular Basis of Cardiovascular Disease*. Philadelphia, Pa: WB Saunders Co. (1998).
16. Bartel, D. P. MicroRNAs: genomics, biogenesis, mechanism, and function. *Cell* **116**, 281–297 (2004).
17. van Rooij, E. *et al*. A signature pattern of stress-responsive microRNAs that can evoke cardiac hypertrophy and heart failure. *Proc. Natl. Acad. Sci. USA.* **103**, 18255-18260 (2006).
18. Sayed, D., Hong, C., Chen, I.Y., Lypowy, J. & Abdellatif, M. MicroRNAs play an essential role in the development of cardiac hypertrophy. *Circ. Res.* **100**, 416-424

(2007).

19. van Rooij, E., Sutherland, L. B., Qi, X., Richardson, J. A., Hill, J., Olson, E. N. Control of stress-dependent cardiac growth and gene expression by a microRNA. *Science* **316**, 575-579 (2007).
20. Yang, B. *et al*. The muscle-specific microRNA miR-1 regulates cardiac arrhythmogenic potential by targeting GJA1 and KCNJ2. *Nat. Med.* **13**, 486-491 (2007).
21. Carè, A. *et al*. MicroRNA-133 controls cardiac hypertrophy. *Nat. Med.* **13**, 613-618 (2007).
22. Lee, D. Y., Deng, Z., Wang, C. H. & Yang, B. B. MicroRNA-378 promotes cell survival, tumor growth, and angiogenesis by targeting SuFu and Fus-1 expression. *Proc. Natl. Acad. Sci. USA.* **104**, 20350-20355 (2007).
23. Glazov, E. A., McWilliam, S., Barris, W. C., Dalrymple, B. P. Origin, evolution, and biological role of miRNA cluster in DLK-DIO3 genomic region in placental mammals. *Mol. Biol. Evol.* **25**, 939-948 (2008).
24. Nakai, A., Suzuki, M. & Tanabe, M. Arrest of spermatogenesis in mice expressing an active heat shock transcription factor 1. *EMBO J.* **19**, 1545–1554 (2000).
25. Inouye, S. *et al*. Impaired IgG production in mice deficient for heat shock transcription factor 1. *J. Biol. Chem.* **279**, 38701–38709 (2004).
26. Chen, J. *et al*. The role of *microRNA-1* and *microRNA-133* in skeletal muscle proliferation and differentiation. *Nat. Genet.* **38**, 228-233 (2006).

Figure Legends

Figure 1: Cardiac hypertrophy and functions after TAC. (**a**-**c**) TAC was induced in adult male WT (**a**), *HSF1*-TG (**b**) and KO (**c**) mice, and echocardiography (ECHO), cardiac catheterization, hematoxylin-eosin staining (H-E) and masson-trichrome staining (MS) were performed 2 (2W) and 4 weeks (4W) later. Representative photographs are shown (scale bars: 200 μm). There were no differences in LV wall thickness, LV cavity and myocardial fibrosis among the sham-operated (Sham) three types of mice. TAC for 2 weeks induced a significant cardiac hypertrophy including the increase in LV wall thickness, decrease of LV cavity and increase in myocardial fibrosis in WT mice. However, LV wall was thicker, cavity was smaller and fibrosis was less in the TG mice whereas LV wall was thinner, cavity was larger, and fibrosis was more in the KO mice than in WT mice. At 4 weeks, LV wall thickness was decreased, cavity was enlarged and myocardial fibrosis was increased compared to those at 2 weeks in WT mice. All these changes were less in TG mice but more in the KO mice. (**d**) Echocardiographic analyses for left ventricular ejection fraction (%LVEF) and end-diastolic LV inner diameter (LVIDd). Data are expressed as mean ± S.E.M. of five mice (n=5). * $p < 0.05$ *vs* Sham; # $p < 0.05$ *vs* 4W in WT mice.

Figure 2: Effects of angiogenesis on cardiac hypertrophy. (**a**) Microvasculature densities. WT, TG and KO mice were subjected to TAC for 4 weeks. Heart sections were immunohistochemically stained with anti vWF antibodies. Representative photographs are shown (original magnification x1000). Sham, sham-operated WT mice. Brown color indicates vWF-positive capillaries. vWF-positive vasculatures were calculated as the

numbers per mm^2 area in LV wall. Data are expressed as mean ± S.E.M. of five hearts (n=5). * $p < 0.05$ *vs* Sham; # $p < 0.05$ *vs* WT with TAC. (**b**) Effects of TNP-470 on cardiac hypertrophy in the TG mice. TG mice were treated with TNP-470 (TNP) or vehicle [9], and subjected to TAC for 4 weeks. Heart sections were stained with H-E and representative photographs from 5 hearts were shown (scale bars: 2 mm). Sham, sham-operated TG mice; TAC, vehicle-treated TG mice with TAC; TNP-TAC, TNP-treated TG mice with TAC. (**c**) Effects of overexpression of *angiopoietin1* (*Ang1*) and *VEGF* in myocardium on cardiac hypertrophy in the KO mice. Adenovirus vectors encoding *Ang1* and *VEGF* were injected into myocardium of the KO mice, and the mice were subjected to TAC for 4 weeks. Heart sections were stained with H-E and representative photographs from 5 hearts were shown (scale bars: 2 mm). Sham, sham-operated KO mice; TAC, vector-injected KO mice with TAC; VEGF+Ang1-TAC, *VEGF* and *Ang1* genes-injected mice with TAC.

Figure 3: Expression of *HIF-1* and *p53* in the heart after TAC. The WT, TG and KO mice were subjected to TAC for 4 weeks. mRNA was extracted from the LV tissues and subjected to a RT-PCR analyses for *HIF-1* (**a**) and *p53* (**b**) expression. *GAPDH* was used as a loading control. Upper, representitive photographs. Expression of *HIF-1* and *p53* were quantified as % of *GAPDH* expression. Data are expressed as mean ± S.E.M. from five mice (n=5). * $p < 0.05$ *vs* sham-operated WT mice; # $p < 0.05$ *vs* WT mice with TAC.

Figure 4: Effects of *HIF-1* and *p53* on cardiac hypertrophy after TAC. Adenovirus vectors encoding *HIF-1*, *p53* and siRNA of *HIF-1* (*HIF-1 siRNA*) or *p53* (*p53 siRNA*), or

empty vectors (Vector) were injected into hearts of the KO (**a-c**) and TG (**d-f**) mice, and the mice were subjected to TAC or sham for 4 weeks. Echocardiography (**a** and **d**, upper) and H-E staining (**a** and **d**, bottom) were used to evaluate cardiac hypertrophy and functions. (**a**) Representative photographs from the KO mice (scale bars: 2 mm). (**b** and **c**) Echocardiographic parameters (LVIDd and %LVEF) were quantitated as mean ± S.E.M. of five KO mice. * $p < 0.05$ *vs* sham; # $p < 0.05$ *vs* TAC-operated mice with vector injection. (**d**) Representative photographs of the TG mice. (**e** and **f**) Quantification of LVIDd and %LVEF. Data are expressed as mean ± S.E.M. of five TG mice. # $p < 0.05$ *vs* TAC-operated mice with vector injection.

Figure 5: Formation of vasculatures by cardiac endothelial cells of microvessels (MEC). MEC were isolated from LV of the WT, TG and KO mice. Vasculature formation experiments were performed as described in Methods. (**a**) Representative photograms of vessel-like tubes from five independent experiments were shown. CT, control, MEC without stimulation; MS, MEC with mechanical stretch stimulation. Total vessels were counted in whole dish. (**b**) Representative RT-PCR analyses for *HIF-1* and *p53* expression of the MEC as in **a**. *GAPGH* was used as loading control. Expression of *HIF-1* and *p53* was quantified as % of *GAPDH* expression. Data are expressed as mean ± S.E.M. of five independent experiments (n=5). * $p < 0.05$ *vs* controls; # $p < 0.05$ *vs* MEC from the WT mice stimulated by mechanical stretch.

Figure 6: Analysis of *miR-378* and *miR-379* in the pressure overloaded hearts. Low-molecular-weight or total RNA was extracted from hearts of the WT, TG and KO

mice subjected to sham or TAC operation for 2 weeks. (**a**) miRNA array expression data. Representative photogram of microarray (*left*) was shown. The expression levels of *miR-378* and *miR-379* were quantified as the fold of expressions in the heart of sham-operated WT mice. (**b**) Northern blot analyses. Expression of *miR-378* and *miR-379* was examined using total RNA of heart tissues from mice as in **a** (*left*) and human (*right*). tRNA was used as loading control. Representative photograms from three independent experiments are shown. NH, heart of human without heart failure; FH, heart of human with heart failure. (**c**) Quantitation of Northern blotting. Expression levels were calculated as the fold of expressions in the heart of sham-operated WT mice. Data are expressed as mean ± S.E.M. from three independent experiments (n=3). * $p < 0.05$ *vs* WT mice with sham operation. (**d**) Effects of *miR-378* and *miR-379* on cardiac hypertrophy and functions. Adult WT mice were subjected to TAC. Two weeks later, the *miR-378* (*378*), siRNA of *miR-379* (*si379*) or empty vector (Vector) were infused into myocardium of the mice. Representative echocardiography (upper), H-E staining (middle) and innunohistochemical staining with anti vWF antibodies (bottom) performed at 4 weeks after TAC were shown (scale bars: 2 mm). Echocardiographic parameters (LVIDd and %LVEF) and vWF-positive capillaries were quantitated as mean ± S.E.M. of five hearts. * $p < 0.05$ *vs* sham with empty vector injection; # $p < 0.05$ *vs* TAC-operated mice with empty vector injection. (**e**) Expression of HSF1. Representative RT-PCR (upper) and Western blot (bottom) analyses for HSF1 in heart of mice as in **d**. *GAPDH* and α-actin were used as loading controls for RT-PCR and Western blotting, respectively.

Fig. 1

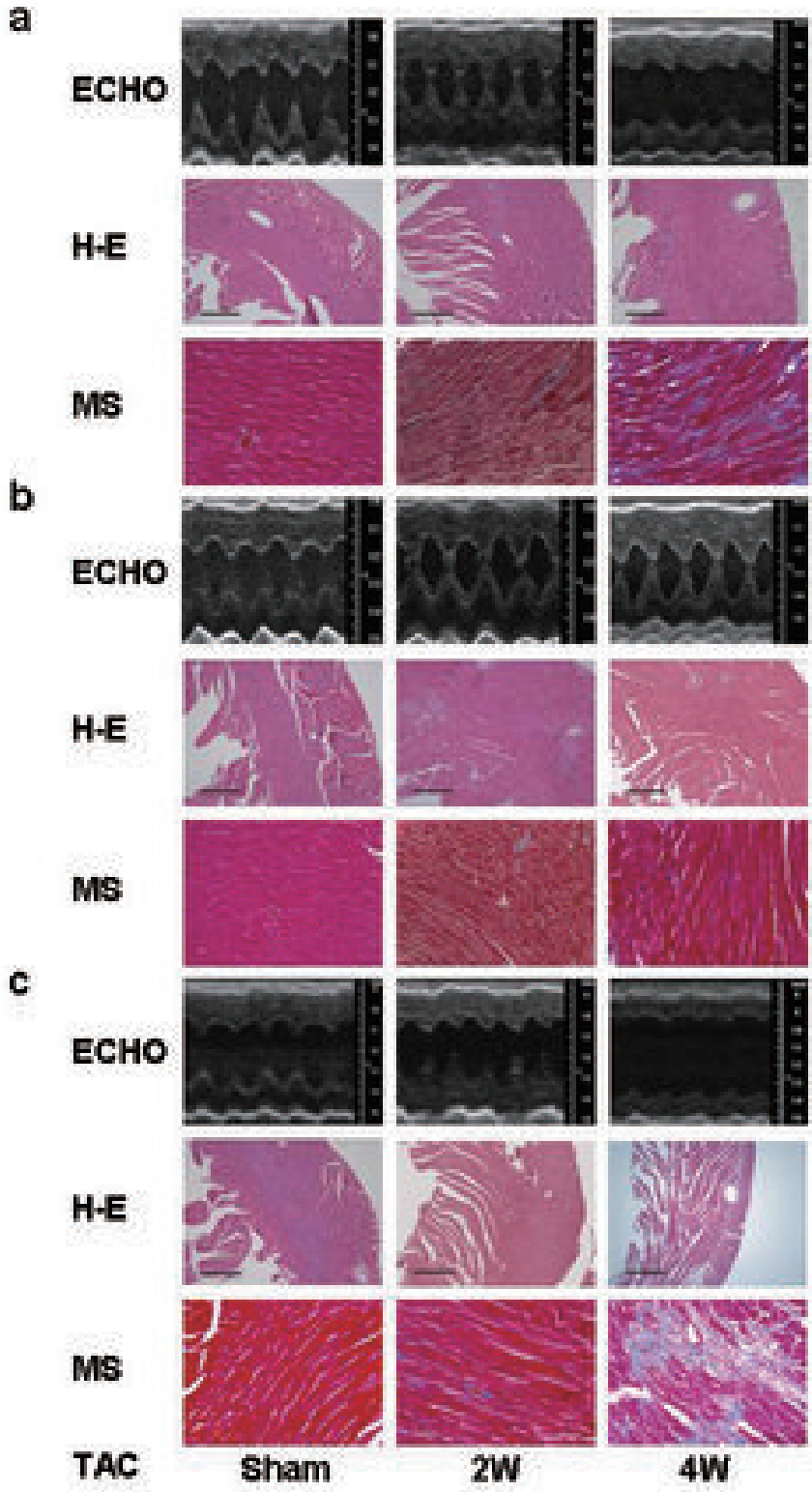
a
ECHO
H-E
MS
b
ECHO
H-E
MS
c
ECHO
H-E
MS
TAC
Sham
2W
4W

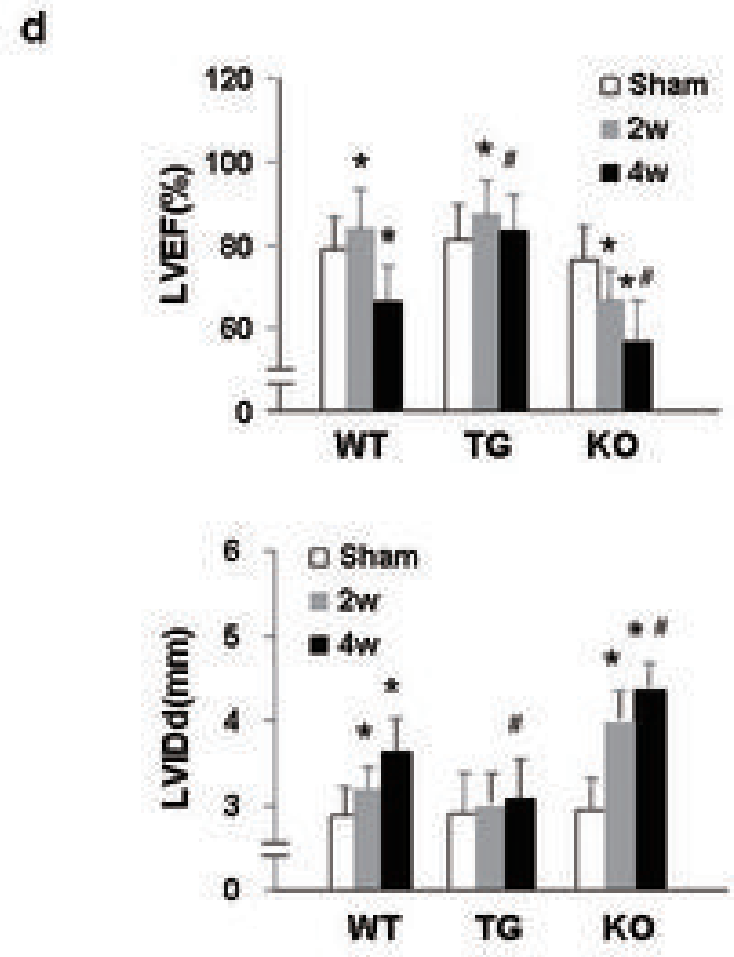
d
LVEF(%)
120
100
80
60
0
Sham
2w
4w
WT
TG
KO
LVIDd(mm)
6
5
4
3
0
Sham
2w
4w
WT
TG
KO

Fig. 2

a

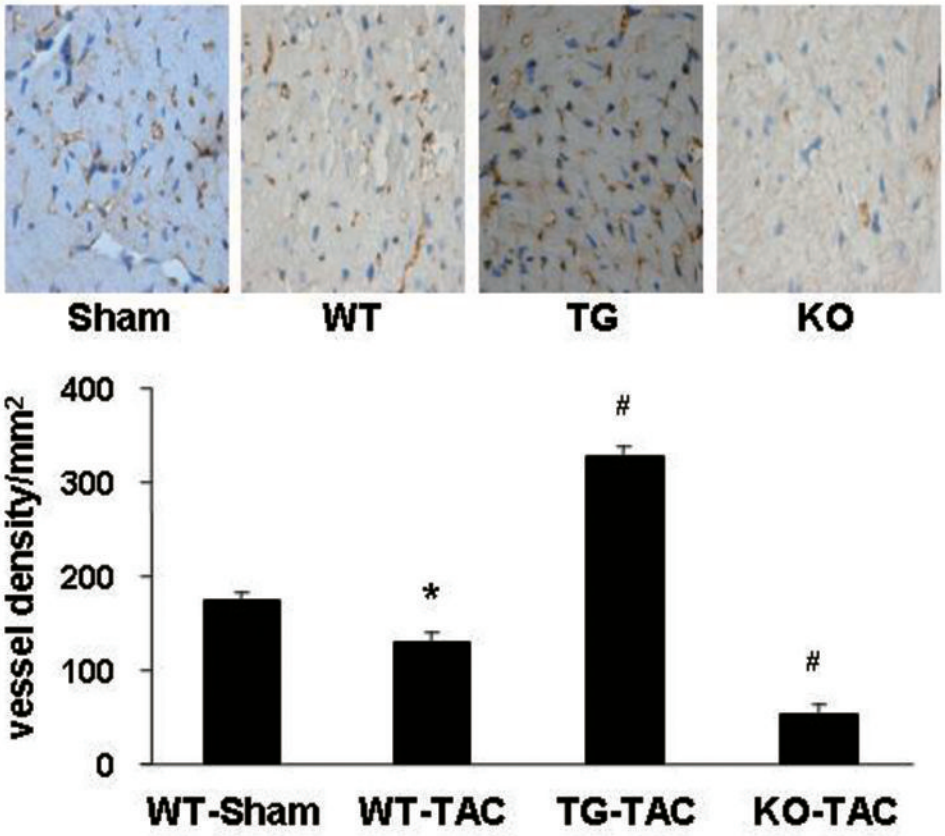
Sham
WT
TG
KO
vessel density/mm2
400
300
200
100
0
*
#
#
WT-Sham
WT-TAC
TG-TAC
KO-TAC

b

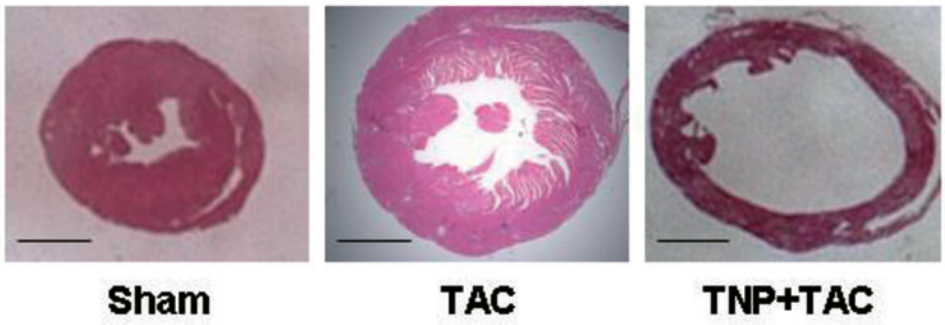
Sham
TAC
TNP+TAC

c

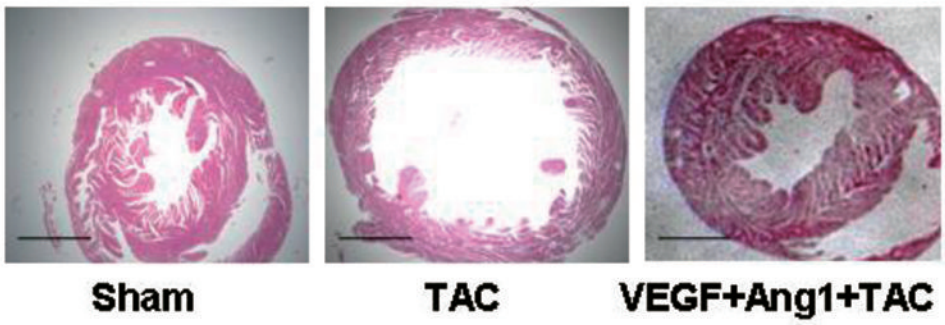
Sham
TAC
VEGF+Ang1+TAC

Fig. 3

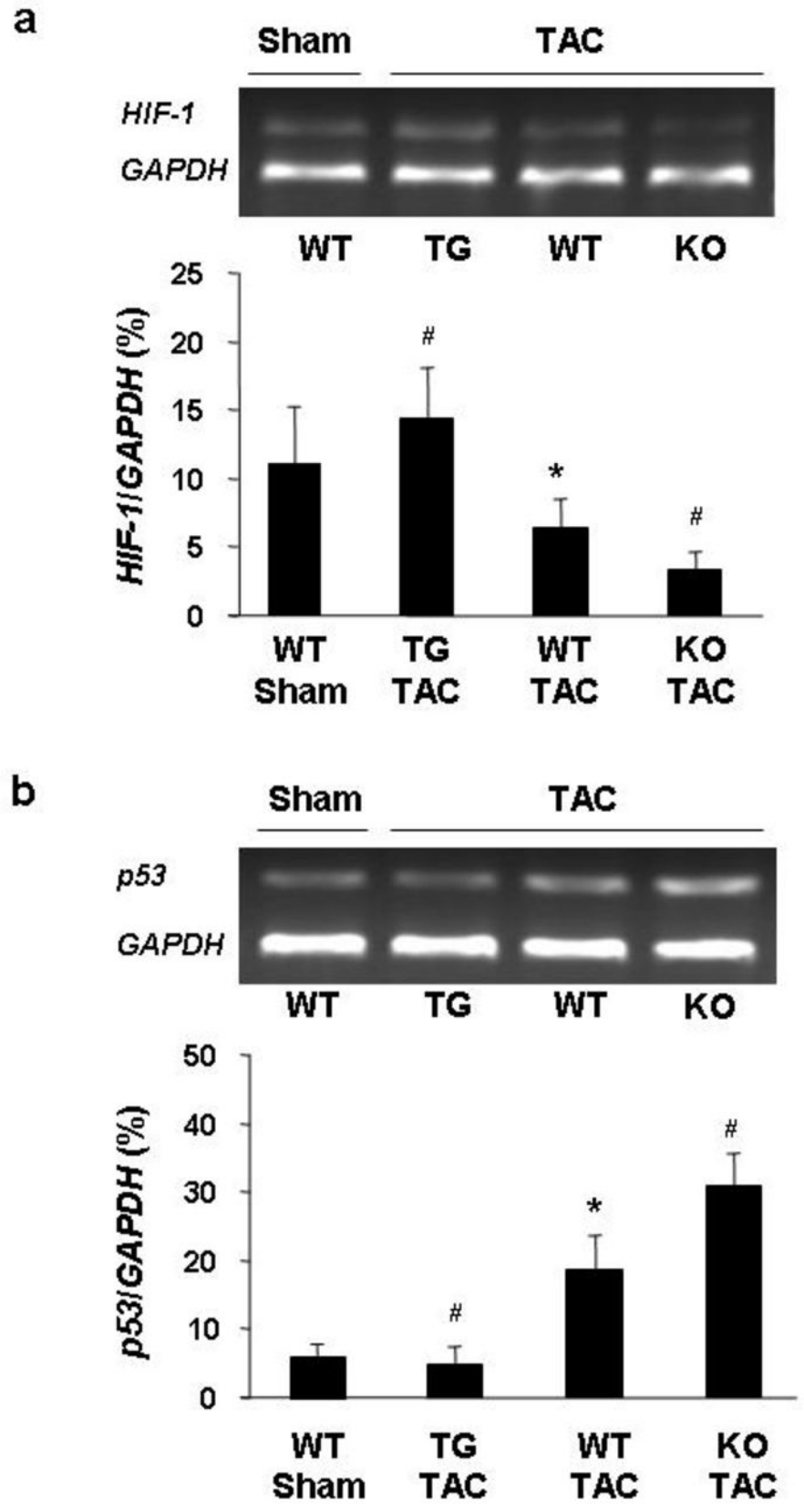
a
Sham
TAC
HIF-1
GAPDH
WT
TG
WT
KO
HIF-1/GAPDH (%)
25
20
15
10
5
0
#
*
#
WT Sham
TG TAC
WT TAC
KO TAC
b
Sham
TAC
p53
GAPDH
WT
TG
WT
KO
p53/GAPDH (%)
50
40
30
20
10
0
#
*
#
WT Sham
TG TAC
WT TAC
KO TAC

Fig. 4

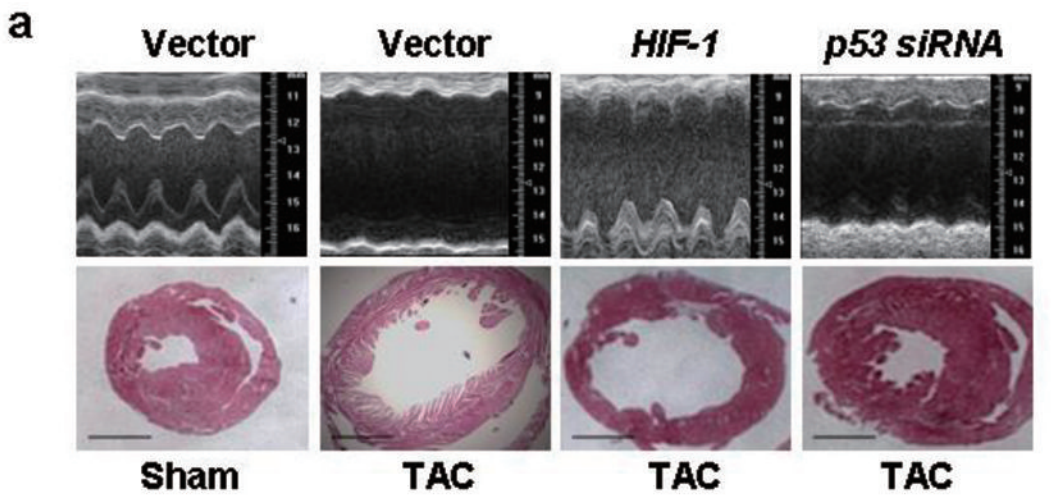
a
Vector
Vector
HIF-1
p53 siRNA
Sham
TAC
TAC
TAC

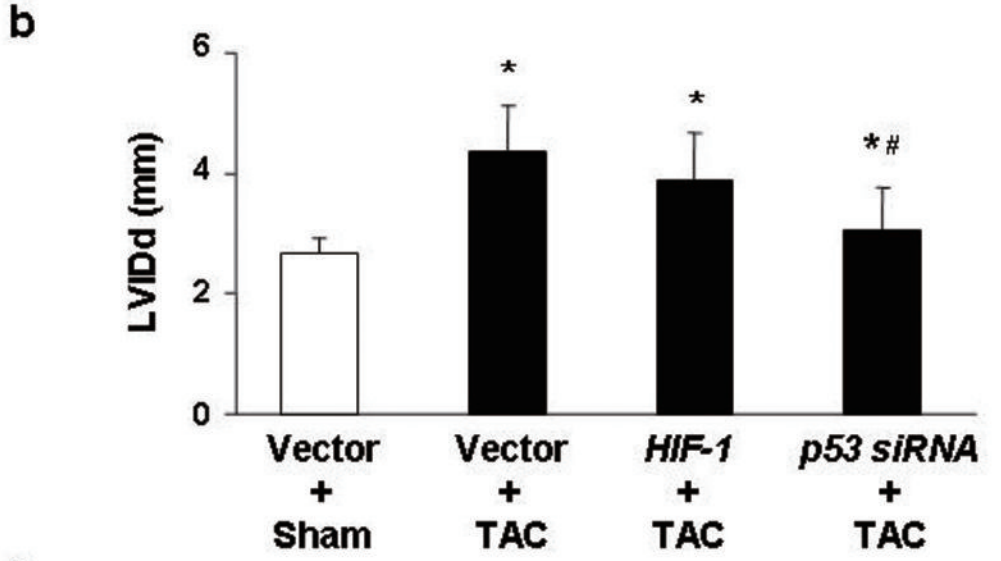
b
LVIDd (mm)
6
4
2
0
*
*
*#
Vector + Sham
Vector + TAC
HIF-1 + TAC
p53 siRNA + TAC

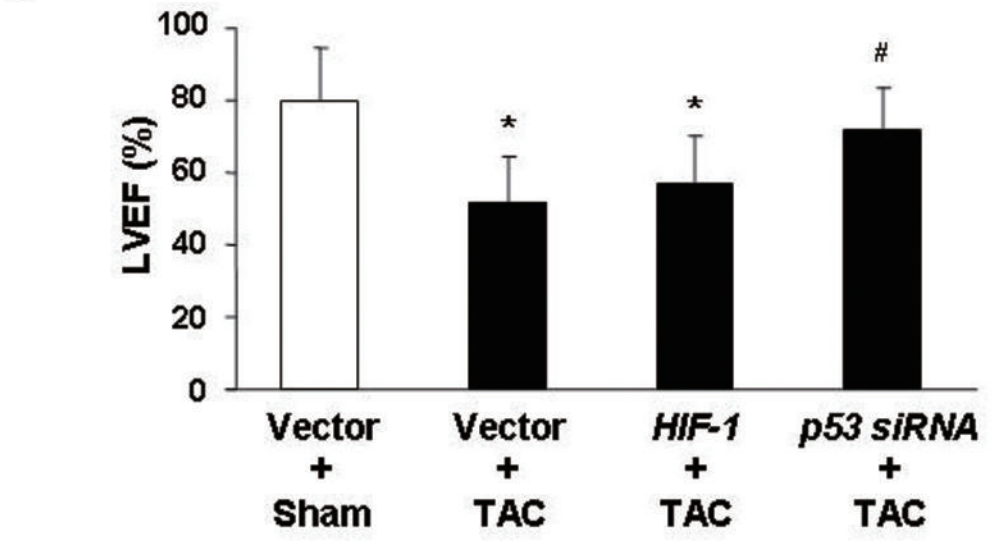
c
LVEF (%)
100
80
60
40
20
0
*
*
#
Vector + Sham
Vector + TAC
HIF-1 + TAC
p53 siRNA + TAC

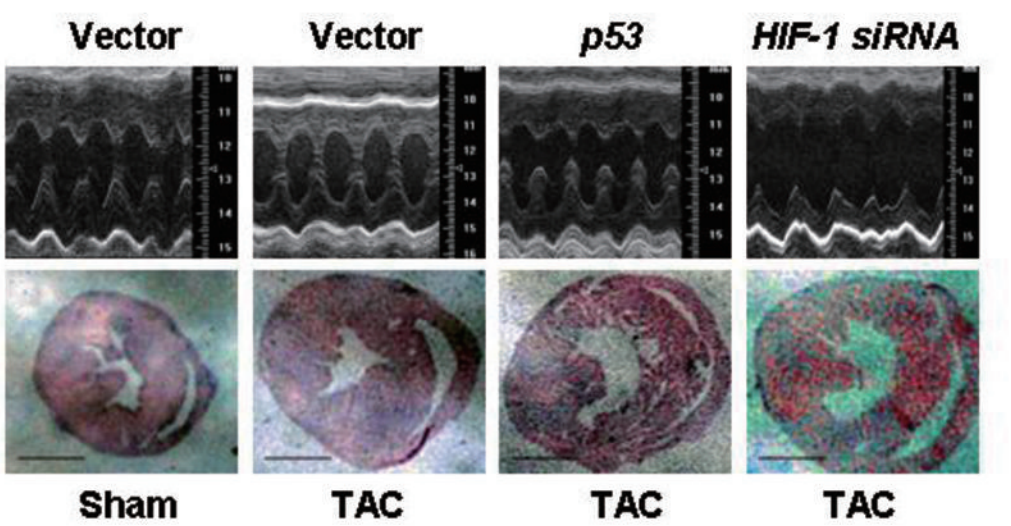
d
Vector
Vector
p53
HIF-1 siRNA
Sham
TAC
TAC
TAC

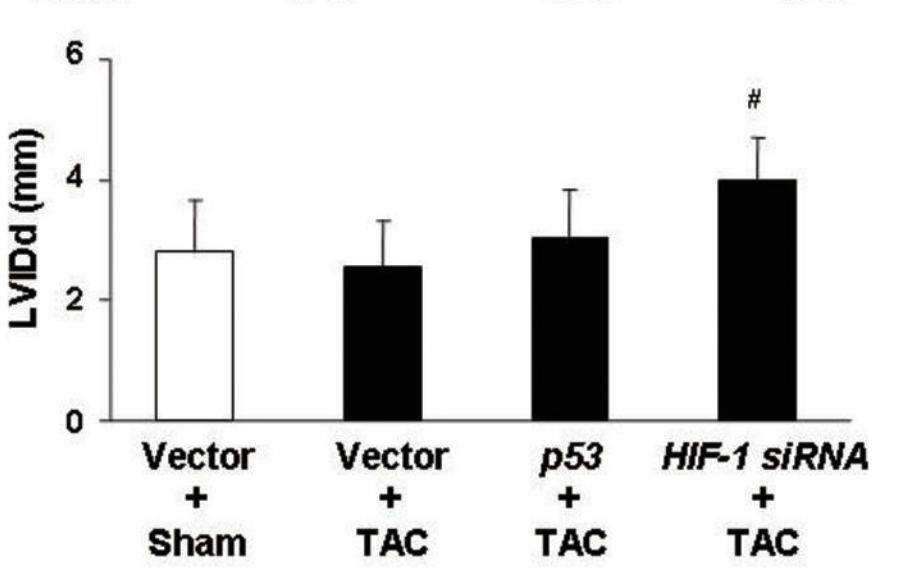
e
LVIDd (mm)
6
4
2
0
#
Vector + Sham
Vector + TAC
p53 + TAC
HIF-1 siRNA + TAC

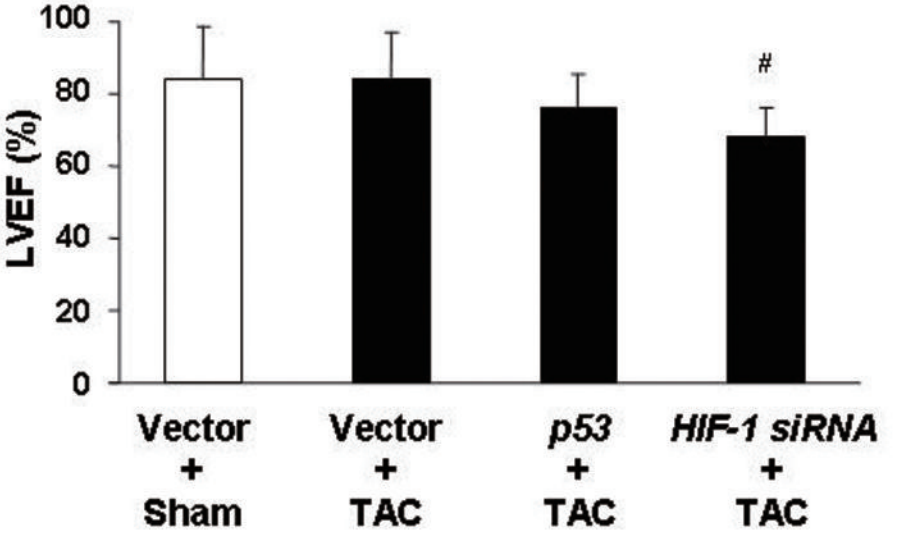
f
LVEF (%)
100
80
60
40
20
0
#
Vector + Sham
Vector + TAC
p53 + TAC
HIF-1 siRNA + TAC

Fig. 5

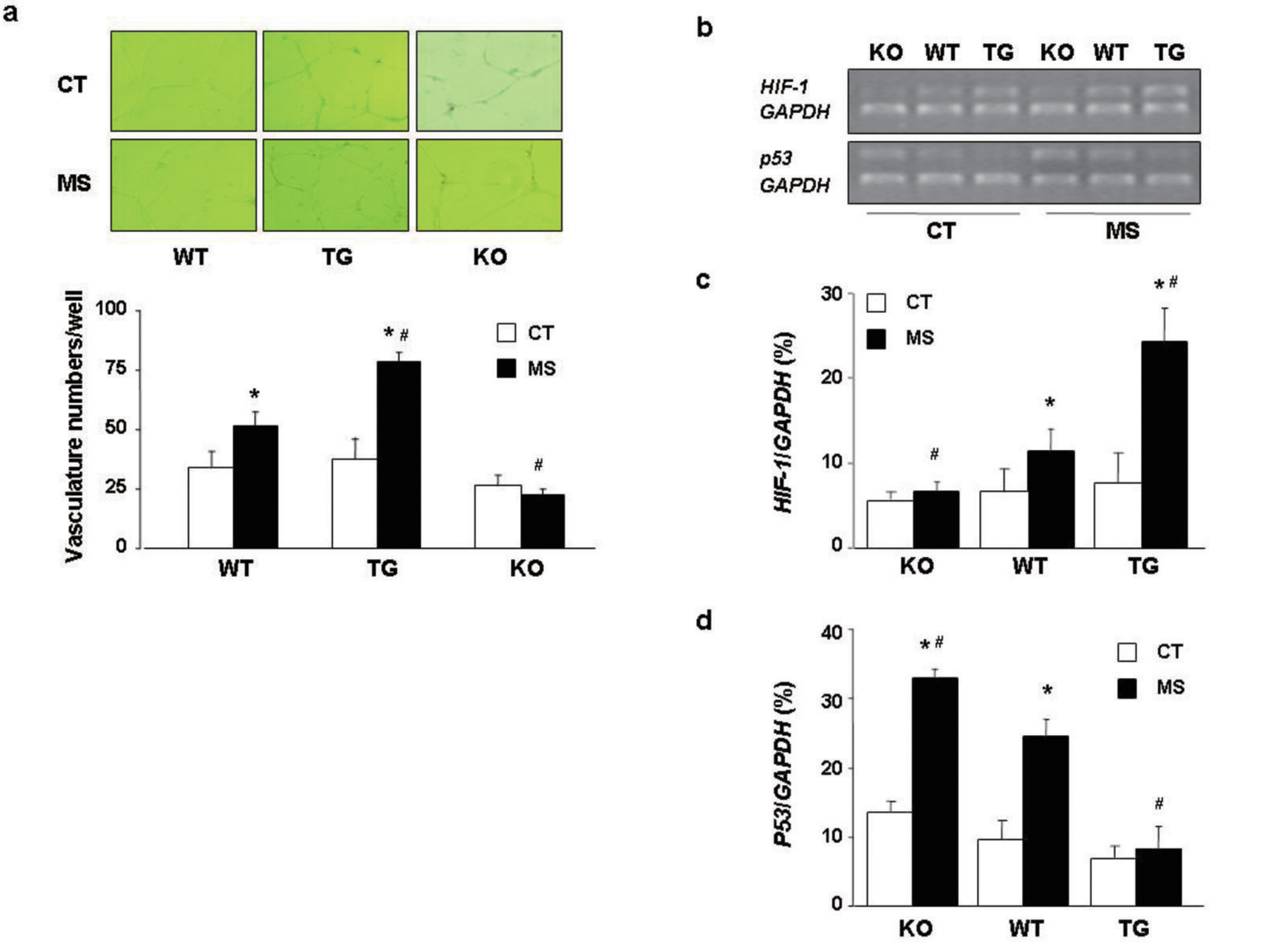
a
CT
MS
WT
TG
KO
Vasculature numbers/well
100
75
50
25
0
CT
MS
b
KO WT TG KO WT TG
HIF-1
GAPDH
p53
GAPDH
CT
MS
c
HIF-1/GAPDH (%)
30
20
10
0
CT
MS
KO
WT
TG
d
P53/GAPDH (%)
40
30
20
10
0
CT
MS
KO
WT
TG

Fig. 6

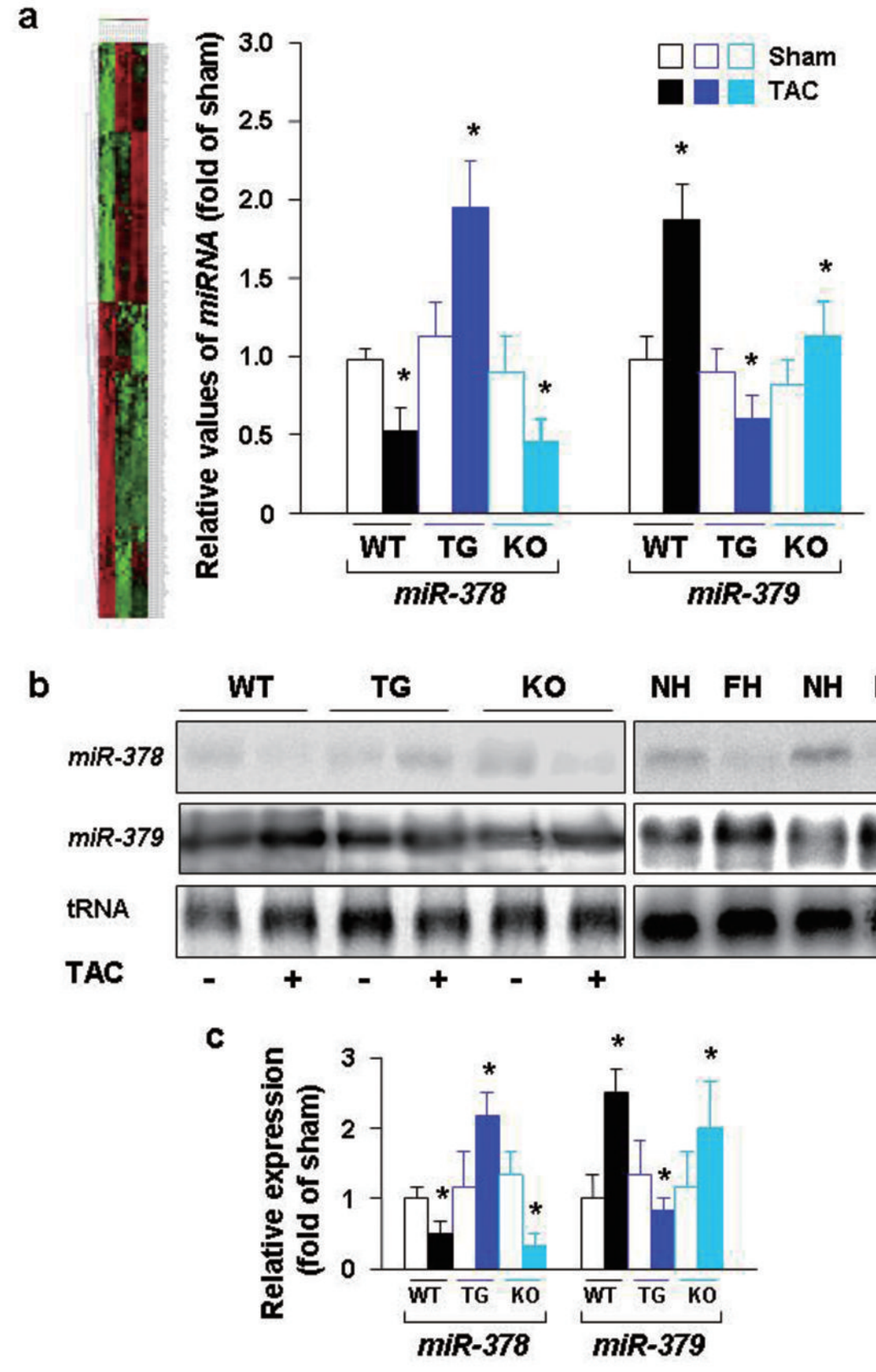
a
Relative values of miRNA (fold of sham)
3.0
2.5
2.0
1.5
1.0
0.5
0
Sham
TAC
WT TG KO
miR-378
WT TG KO
miR-379
b
WT TG KO NH FH NH FH
miR-378
miR-379
tRNA
TAC
- + - + - +
c
Relative expression (fold of sham)
3
2
1
0
WT TG KO
miR-378
WT TG KO
miR-379
d
Vector
Vector
378
si379
Sham
TAC
TAC
TAC
LVID;d(mm)
5
4
3
0
Vector + Sham
Vector + TAC
378 + TAC
si379 + TAC
LVEF(%)
100
80
60
0
Vector + Sham
Vector + TAC
378 + TAC
si379 + TAC
Vessel density/mm2
400
300
200
100
0
Vector + Sham
Vector + TAC
378 + TAC
si379 + TAC
e
HSF-1
GAPDH
HSF-1
Actin
Vector + Sham
Vector + TAC
378 + TAC
si379 + TAC